Research Square

Preprints are preliminary reports that have not undergone peer review.
They should not be considered conclusive, used to inform clinical practice,
or referenced by the media as validated information.

Harnessing the Biogeochemical Iron Cycle for Green Chemical Engineering and Environmental Geo-Remediation

D. Jayarajan
Assam down town University
S. Sivaprakash
St. Joseph's College of Arts and Science (Autonomous)
R. Sagayaraj
sagayaraj@sjctnc.edu.in

St. Joseph's College of Arts and Science (Autonomous)

Systematic Review

Keywords: iron cycle, geo-remediation, green chemistry, zero-valent iron, iron-reducing bacteria, biogenic minerals, circular economy

Posted Date: November 25th, 2026

DOI: https://doi.org/10.21203/rs.3.rs-11745788/v1

License: This work is licensed under a Creative Commons Attribution 4.0 International License.
Read Full License

Additional Declarations: No competing interests reported.

Abstract

Iron is the most abundant redox-active transition metal in Earth's crust, and its biogeochemical cycle couples microbial metabolism, mineral transformation, and the fate of carbon, nutrients, and contaminants. This review synthesizes research published between 2021 and 2025 on how this cycle can be harnessed deliberately for green chemical engineering and geo-remediation. We (i) summarize the redox, mineralogical, and microbial controls on iron cycling; (ii) evaluate iron-based remediation technologies, including zero-valent iron, green-synthesized nanoparticles, biogenic iron minerals, Fenton and persulfate systems, permeable reactive barriers, and bioelectrochemical systems; (iii) compare their performance across contaminant classes in consolidated tables and figures; and (iv) identify the constraints imposed by passivation, scale-up, ecotoxicity, and life-cycle impact. The literature indicates that biogenic and bio-inspired iron materials can approach the removal performance of conventional iron-based treatments for arsenic, chromium, nitrate, and chlorinated solvents with lower reagent and energy demand, although field-scale evidence remains scarce. We propose a decision framework and identify research priorities centered on controlling mineral aging, sourcing iron circularly, and standardizing reporting. Iron-cycle-informed design offers a credible route to low-carbon remediation that is consistent with the principles of green chemistry.

1. Introduction

Iron is the fourth most abundant element in Earth's crust and participates in both biological and chemical processes [1]. Its cycling between Fe(II) and Fe(III) is driven by abiotic reactions and by microorganisms, and it influences ocean productivity, carbon storage, greenhouse gas emissions, and the fate of nutrients, toxic metals, and metalloids [2]. Recent work shows that iron oxidation and reduction can occur cyclically or simultaneously in many environments and that these processes overlap in space and may compete [2, 3]. Understanding the reactivity of Fe(II) in aqueous, ligand-bound, mineral, and sorbed forms is therefore central to predicting how iron regulates other element cycles in natural and engineered systems [1].

Iron minerals strongly influence the fate of carbon. They stabilize soil organic carbon through adsorption, co-precipitation, and aggregation, yet redox cycling can also drive carbon turnover: microbial Fe(II) oxidation tends to stabilize carbon, whereas chemical Fe(II) oxidation and Fe(III) reduction are coupled with its degradation [4–6]. A meta-analysis of 3,395 soil profiles indicates that Fe–Al oxides play an important role in global soil carbon stabilization and stocks [7], and studies of wetland soils show that the balance between iron-mediated carbon mineralization and preservation responds to additions of iron oxide and carbon [8]. Associations between iron (hydr)oxides and organic matter also alter the binding of metal(loid)s and thereby control their immobilization and remobilization [9, 10].

These couplings are sensitive to environmental change. In thawing permafrost peatlands, reductive dissolution of Fe(III) minerals releases iron-bound organic carbon, and microbial iron cycling promotes carbon dioxide and methane production before the permafrost has thawed completely [11]. Iron may

also contribute to methane removal: anaerobic methanotrophic archaea have been shown to respond to ferrihydrite, an Fe(III) mineral, in long-term cultures [12]. Together, these observations show that shifts in redox conditions can turn iron from a sink into a source of carbon and greenhouse gases.

The same redox processes govern contaminant behavior. Dissimilatory iron- and arsenic-reducing bacteria promote the mobilization of arsenic and Fe(II) in sediments and groundwater [13], and iron also offers a route to resource recovery: Fe(II) combines with phosphate to form vivianite, which has been studied as a means of recovering phosphorus from wastewater and sludge [14, 15]. Heavy metal(loid) contamination of agricultural soils is widespread [16], and remediation technologies for contaminated soils have been reviewed extensively [17, 18]. Iron-based materials are widely investigated for treating soil, wastewater, and groundwater contaminated with heavy metals, and sulfidation and biochar supports are reported to improve removal efficiency and stability [19–27]. Iron sulfides and sulfidated zero-valent iron (ZVI) can also activate persulfate for the degradation of organic contaminants [20, 28, 29].

Green chemistry offers a design framework for such technologies. It rests on the 12 Principles of Green Chemistry formulated by Anastas and co-workers, which emphasize waste prevention, safer chemicals, and energy efficiency [30]. In this context, plant-based synthesis of nanoscale ZVI (nZVI) replaces toxic reductants and can lower energy consumption [31–33], and reviews of modified nZVI describe how modification strategies address aggregation and surface passivation [34]. Combining nZVI with anaerobic bacteria is another route explored for in-situ groundwater remediation [35]. Iron-rich industrial by-products add a circular dimension: steel slag is increasingly regarded as a co-product with potential uses in remediation, although heavy metal leaching poses risks [36], and recycled smelter slags have been reviewed for water and wastewater treatment [37].

Despite this progress, field-scale performance and durability are less well understood than laboratory behavior. Reviews of permeable reactive barriers (PRBs) based on ZVI show that corrosion products and mineral precipitates strongly influence long-term reactivity and that hydraulic performance and clogging limit service life [38, 39]. Studies from geochemistry, microbiology, environmental engineering, and materials science are rarely integrated, and few syntheses link the mechanisms of the biogeochemical iron cycle to engineering design.

This review addresses these gaps. Section 2 describes the controls on the biogeochemical iron cycle, Section 3 evaluates green engineering routes built on those controls, Section 4 compares performance, environmental sensitivity, and sustainability across routes, and Section 5 discusses durability, risk, scale-up, and a decision framework. Section 6 presents the conclusions.

2. Fundamentals of the Biogeochemical Iron Cycle

2.1 Redox and mineral controls

Fe(II) is soluble under anoxic, acidic to neutral conditions, whereas Fe(III) precipitates as oxyhydroxides such as ferrihydrite, goethite, and lepidocrocite [1, 40]. Ferrihydrite transforms into more crystalline phases through Fe(II)-catalyzed recrystallization, a process that governs the sequestration or release of co-precipitated elements [40, 41]. Mixed-valence minerals, including magnetite, green rust, siderite, and vivianite, act as both sinks and reductants for contaminants [14, 15, 42]. Table 1 summarizes the main iron phases and their roles in contaminant control.

Table 1
Principal iron minerals in the biogeochemical iron cycle and their remediation roles.

Mineral	Composition / valence	Redox role	Contaminant interactions	Refs
Ferrihydrite	Fe(III) oxyhydroxide, poorly crystalline	Microbial electron acceptor; precursor phase	Sorption and co-precipitation of As, P	[1, 40, 41]
Goethite, lepidocrocite	Fe(III) oxyhydroxides	Electron acceptors; Fe(II)-catalyzed transformation	Sorption of metals and oxyanions	[1, 40]
Magnetite	Mixed Fe(II)/Fe(III) oxide	Reductant and electron conduit	Reduction of Cr(VI), U(VI)	[42]
Green rust	Layered Fe(II)–Fe(III) hydroxide	Strong reductant	Reduction of Cr(VI), nitrate	[42]
Siderite	Fe(II) carbonate	Fe(II) sink and reductant	Cr immobilization	[42]
Vivianite	Fe(II) phosphate	Fe(II) and P reservoir	Phosphorus recovery	[14, 15]
Mackinawite and related FeS	Fe(II) sulfide	Reactive sulfide phase	Sulfidation of ZVI; metal precipitation	[20, 21]

Table 1 shows that reactivity follows redox state and crystallinity. Poorly crystalline ferrihydrite offers the largest sorption capacity but is also the phase most prone to transformation, whereas mixed-valence phases such as magnetite and green rust combine structural Fe(II) with electron conduction and therefore act as reductants [1, 40–42]. Sulfide phases extend this logic to sulfidated ZVI [20, 21]. These phase properties determine the contaminant pathways compared in Tables 4 and 5.

2.2 Microbial drivers

Figure 1 shows how these processes fit together. Dissimilatory iron-reducing bacteria such as *Geobacter* and *Shewanella* transfer electrons to Fe(III) minerals via outer-membrane cytochromes and conductive nanowires [43–48]. Neutrophilic and nitrate-dependent Fe(II) oxidizers close the cycle under microaerobic and anoxic conditions [2, 49–52]. Electron shuttles, including humic substances and flavins, extend reduction to otherwise inaccessible minerals [45]. Iron-based syntrophy with

methanogens and anaerobic methane oxidizers links iron to greenhouse gas control [12]. Table 2 groups the microbial functional guilds relevant to engineering.

Table 2
Microbial guilds that drive iron redox transformations.

Guild	Examples	Metabolism	Engineering relevance	Refs
Dissimilatory Fe(III) reducers	*Geobacter*, *Shewanella*	Fe(III) respiration via cytochromes and nanowires	Reductive immobilization; biogenic minerals; electrodes	[43–45, 47, 48]
Neutrophilic Fe(II) oxidizers	*Gallionella*, *Sideroxydans*	Microaerobic Fe(II) oxidation	Oxide formation, arsenic trapping	[2, 51, 52]
Nitrate-dependent Fe(II) oxidizers	Denitrifying consortia	Fe(II)-coupled nitrate reduction	Nitrate removal; N2O risk	[2, 49–51]
Phototrophic Fe(II) oxidizers	Photoferrotrophs	Light-driven Fe(II) oxidation	Anoxic Fe(III) regeneration	[2]
Electron-shuttle producers	Humic and flavin mediators	Extracellular electron shuttling	Extends reduction to recalcitrant minerals	[45]
Fe-linked methane cyclers	Methanogens, methanotrophs	Iron-coupled methane cycling	Greenhouse-gas control	[12]

Table 2 distinguishes guilds that raise Fe(II) from those that regenerate Fe(III). Reducers such as *Geobacter* and *Shewanella* generate Fe(II) and can mobilize sorbed arsenic or phosphorus, whereas microaerophilic, nitrate-dependent, and phototrophic oxidizers rebuild Fe(III) oxides that re-immobilize them [2, 43–45, 49–51]. Which direction dominates depends on electron-donor supply, oxygen, and nitrate (Table 6), and electron shuttles accelerate the reduction of recalcitrant minerals [45]. The iron–methane guilds connect these controls to greenhouse gas outcomes [12].

Figure 1 depicts two coupled processes. The horizontal exchange between Fe(III) minerals and Fe(II) phases is set by microbial reduction and by oxidation with oxygen, nitrate, or light [2, 43–45, 49–51]. The vertical branches show that sorption and co-precipitation operate mainly on the Fe(III) side, whereas reduction and radical oxidation operate on the Fe(II) side [28, 40–42, 53]. The engineering levers (electron donors, aeration, electrodes, ZVI, and Fenton reagents) work by shifting the balance between the two sides, which is why the parameters in Table 6 control remediation outcomes [45].

3. Green Engineering Routes Based on the Iron Cycle

Engineered use of the iron cycle follows three design strategies: supplying reactive iron phases, steering redox conditions so that iron cycles in situ, and recovering iron from waste streams for reuse. Each strategy can be assessed against green chemistry criteria such as waste prevention, safer reagents, energy efficiency, renewable or recovered feedstocks, and design for degradation [28, 31, 34, 38]. The

routes below progress from engineered materials (Sections 3.1 and 3.2) to process-level coupling (Section 3.3), field implementation (Section 3.4), and circular sourcing (Section 3.5).

3.1 Zero-valent iron and its green-synthesized variants

Nanoscale zero-valent iron (nZVI) consists of a metallic Fe(0) core surrounded by an iron oxide shell, and contaminant reduction proceeds by electron transfer through or around this shell [19, 25, 26, 34, 54, 55]. Cr(VI) is reduced to Cr(III) and precipitated, nitrate is reduced to ammonium or nitrogen, and chlorinated solvents undergo reductive dechlorination [19, 34, 54, 56–59]. Two limitations recur in the recent literature. Magnetic attraction causes particles to aggregate and reduces the accessible surface area, and the oxide shell thickens over time, passivating the core and diverting electrons to water reduction and hydrogen evolution [19, 26, 34, 54, 58, 60, 61]. Both effects shorten the effective service life and increase the iron dose required [35, 39, 61].

Green synthesis addresses hazard and dispersion simultaneously. Polyphenols in plant and agro-waste extracts reduce dissolved Fe(II) or Fe(III) and adsorb onto the particle surface as capping agents, which avoids borohydride and limits aggregation [31–34]. Microbial exudates and enzymes offer a further low-energy route [31, 34]. Because organic capping and incomplete reduction often yield particles with lower Fe(0) content than borohydride-synthesized nZVI, part of the removal reported for green materials arises from adsorption and complexation rather than reduction alone, and this distinction should be reported explicitly [31, 32, 34]. Table 3 compares the main routes and their limitations.

Table 3
Green synthesis and modification routes for iron materials.

Route	Reductant / modifier	Main benefit	Limitation	Refs
Plant-extract nZVI	Polyphenols from leaves and tea	Avoids borohydride; capping	Batch variability	[31, 34]
Agro-waste-mediated synthesis	Waste biomass extracts	Low cost, waste valorization	Feedstock heterogeneity	[31, 34]
Microbial exudate synthesis	Biomolecules and enzymes	Mild conditions	Slow, difficult to scale	[31, 34]
Sulfidation	Sulfide or thiosulfate	Selectivity, longevity	Dose optimization	[20, 21, 28]
Biochar or clay supports	Porous carriers	Dispersion, reduced aggregation	Support cost and aging	[22–24]

Table 3 indicates that greener synthesis acts mainly on particle dispersion and surface reactivity. Capping with polyphenols and other biomolecules reduces aggregation, which increases the accessible reactive surface and helps to explain the high removal reported for green nZVI in Table 4 [31, 34].

Sulfidation and carbon supports address the same weaknesses from a different direction. Sulfidation forms Fe–S phases that suppress hydrogen evolution and increase selectivity for chlorinated solvents and arsenic, but performance is sensitive to the sulfur dose and the sulfidation method [20, 21, 28, 62–64]. Biochar or clay supports disperse the particles and add sorption capacity, at the cost of an additional material that must be sourced and that also ages [22–24, 27, 65–67]. Both modifications improve selectivity and dispersion but introduce dose and cost parameters that must be optimized [20, 21, 28].

3.2 Biogenic iron minerals and stimulated iron redox cycling

When iron-reducing bacteria respire Fe(III) oxides, the resulting Fe(II) reacts with the remaining Fe(III) phases and with dissolved bicarbonate, phosphate, and sulfide to form magnetite, siderite, vivianite, and iron sulfides [14, 15, 42, 51]. These phases immobilize As, U, and Cr through reductive precipitation, structural incorporation, and surface complexation [14, 15, 42, 51, 68, 69]. Biogenic magnetite is also magnetically separable, and vivianite forms a recoverable phosphorus product, which links remediation to resource recovery [14, 15, 51]. Because the product depends on the electron donor, pH, and the concentrations of bicarbonate and phosphate, the target phase can in principle be steered by controlling the solution chemistry [14, 15, 42, 51].

At the process scale, deliberate alternation of reducing and oxidizing conditions in constructed wetlands and bioreactors uses iron as an internal redox mediator. Reducing phases mobilize Fe(II) and support nutrient and metalloid transformations, whereas oxidizing phases regenerate Fe(III) oxides that recapture arsenic and phosphorus [49, 51]. Bioaugmentation with iron reducers can accelerate start-up in contaminated media [49, 51], but the approach remains sensitive to temperature, carbon supply, and competing electron acceptors, which explains the seasonal variability reported for field-like systems [49, 51].

3.3 Advanced oxidation and electrochemical coupling

In Fenton chemistry, Fe(II) activates hydrogen peroxide to produce hydroxyl radicals, and the rate-limiting step is the reduction of Fe(III) back to Fe(II). Homogeneous systems therefore require acidic pH and generate iron sludge, which is the main green chemistry penalty of the classical process [28, 53, 70–73]. Heterogeneous catalysts on waste-derived supports, iron-mineral photo-Fenton systems, and persulfate activation widen the usable pH range and reduce sludge, while in-situ generation of Fe(II) lowers reagent use [28, 53, 70, 71, 74–78]. Pharmaceutical residues and dyes are the main targets, and iron leaching and oxidant dose are the principal parameters to control [28, 53, 70, 71, 79].

Bioelectrochemical systems extend iron cycling by replacing chemical donors or acceptors with electrodes. Electrodes can supply electrons to iron reducers, drive Fe(II) regeneration, or serve as the electron acceptor for oxidizers, and the same cells can recover energy while treating metals and

organics [44, 45, 80, 81]. Their main constraints are electrode cost, the conductivity of the medium, and the scale-up of reactor design [44, 45, 82].

3.4 Permeable reactive barriers and in-situ geo-remediation

Iron-based permeable reactive barriers (PRBs) and injected colloidal iron are the main field-scale deployments. A PRB intercepts a plume with reactive media, so its performance depends on residence time, hydraulic conductivity, and the reactivity of the iron over years [38, 39, 54]. Carbonate, hydroxide, and iron sulfide precipitates form in the media as groundwater chemistry interacts with the iron; they reduce porosity (clogging), cause flow bypass, and passivate the iron surface [38, 39, 54]. Injection of colloidal or nanoscale iron can reach source zones that a barrier cannot, but its transport and reactivity depend on particle stabilization and aquifer heterogeneity [38, 39, 54]. Recent studies therefore emphasize long-term reactivity, hydraulic performance, and monitoring protocols rather than initial removal alone [38, 39, 54].

3.5 Circular sourcing and integrated treatment trains

Steel slag, mine-drainage sludge, and water-treatment residuals are iron-rich by-products that can serve as feedstocks for reactive media, supports, and catalysts [36, 37, 83]. Using them lowers embodied impacts and diverts waste, but their composition varies and leaching of co-occurring metals must be assessed [36, 37]. Life-cycle and techno-economic assessments suggest that the benefit depends on transport distance, activation energy, and replacement frequency [102, 103]. Combining routes can offset the weaknesses of single routes, for example by pairing biogenic phases for stable immobilization with ZVI for rapid reduction, or by controlling redox electrochemically within a wetland [14, 15, 44, 45, 49, 51].

4. Results: Comparative Performance and Trends

4.1 Removal performance across approaches

Reported removal efficiencies cluster by mechanism and contaminant (Table 4, Fig. 2). Green-synthesized nZVI frequently achieves high removal of Cr(VI), nitrate, and dyes in batch studies, because polyphenol coatings limit aggregation and supply additional reducing capacity [31, 34, 49, 84–86]. Sulfidation shifts ZVI toward the selective reduction of chlorinated solvents and arsenic by suppressing hydrogen evolution and altering surface sites [20, 21, 28, 54]. Biogenic magnetite and siderite achieve high but slower removal of As, U, and Cr through reductive precipitation and sorption [13–15, 42, 51, 87, 88], and vivianite adds a pathway for phosphorus recovery [14, 15]. Coupled microbial iron cycling in wetlands and bioreactors delivers moderate to high removal of nitrogen, phosphorus, and arsenic, but with seasonal variability [13, 49, 51, 88]. Fenton and persulfate systems on waste-derived supports achieve very high degradation of organics but are constrained by pH control and sludge [28, 53, 70, 71], and bioelectrochemical systems show promising but scale-limited performance [44, 45, 89, 90].

Table 4
Summary of iron-based remediation approaches, targets, and reported performance ranges (2021–2025).

Approach	Main targets	Typical removal reported	Key mechanism	Principal limitation	Refs
Green-synthesized nZVI	Cr(VI), nitrate, dyes	80–99%	Reduction, adsorption	Aggregation, oxide shell	[19, 20, 31–34, 49, 54, 58, 59, 84–86]
Sulfidated ZVI	Chlorinated solvents, As	70–99%	Selective reduction	Sulfur dose optimization	[20, 21, 28, 62–64]
Biogenic magnetite/siderite	As, U, Cr	70–98%	Reductive precipitation, sorption	Slow kinetics	[13–15, 42, 51, 68, 69, 87, 88]
Fe-cycling wetlands/bioreactors	N, P, As	60–95%	Coupled microbial Fe redox	Seasonality	[13, 49, 51, 88]
Fenton/persulfate (green supports)	Organics, pharmaceuticals	85–99%	Radical oxidation	pH, sludge	[28, 53, 70–73, 75, 78, 91]
Bioelectrochemical systems	Metals, organics	60–95%	Electrode-mediated Fe redox	Scale-up	[44, 45, 82, 89, 90, 92–96]
PRBs/injected colloids	Plumes: Cr, TCE, As	Field-dependent	Reduction, precipitation	Clogging, aging	[38, 39, 54]

Table 4 and Fig. 2 should be read together. Removal efficiency depends on the mechanism (reduction, sorption, or oxidation), on the iron dose and form, and on the controls listed in Table 6. Approaches with fast abiotic kinetics (ZVI and Fenton) cluster at the high end, whereas coupled microbial systems trade peak rate for lower reagent demand and regenerative capacity [13–15, 19–21, 28, 31, 34, 42, 44, 45, 49, 51, 53, 54, 70, 71, 84–90].

Figure 2 shows that upper-bound removal is similar for most approaches (95–99%), whereas lower bounds differ more, with biological and electrochemical systems at the low end. This wider spread is consistent with their sensitivity to temperature, season, and electron-donor supply (Table 6) [13, 44, 45, 49, 51, 88–90]. The high ceiling for Fenton-type systems reflects the degradation of organics rather than the immobilization of metals, so it cannot be compared directly with the metal-focused approaches [28, 53, 70, 71]. Because the ranges derive from batch and column studies, they describe potential rather than field performance [19, 35, 38, 39, 54].

4.2 Contaminant-specific mechanisms

The dominant mechanism depends on the contaminant and the iron phase involved (Table 5). Cr(VI) and chlorinated solvents are removed mainly by electron transfer from Fe(0) or structural Fe(II) [20, 42, 54, 56, 84–86], whereas arsenic and phosphorus are controlled by sorption and co-precipitation, which depend on the stability of iron oxides during recrystallization [1, 13–15, 40, 41, 87, 88]. Uranium is immobilized by reduction to U(IV) on magnetite and related minerals [42], and nitrate is removed by Fe(0) reduction or by Fe(II)-coupled biological denitrification, the latter with a risk of N_2O formation [2, 34, 49–51].

Table 5
Dominant mechanisms and iron phases by contaminant class.

Contaminant	Dominant mechanism	Key iron phases	Main risk or uncertainty	Refs
Cr(VI)	Reduction to Cr(III), precipitation	nZVI, siderite, Fe(II) minerals	Re-oxidation of Cr(III)	[42, 51, 56, 57, 59, 62, 84–86, 94, 97]
As(III/V)	Sorption, co-precipitation	Ferrihydrite, magnetite, sulfidated ZVI	Release during recrystallization	[1, 13, 40, 41, 87, 88, 98]
Chlorinated solvents	Reductive dechlorination	Sulfidated ZVI, PRB iron	Passivation, aging	[20, 21, 28, 38, 39, 54, 99]
Nitrate	Chemical or Fe(II)-driven biological reduction	nZVI, Fe(II) with denitrifiers	N2O, ammonium formation	[2, 34, 49–51, 58, 100]
Uranium	Reduction to U(IV)	Magnetite, green rust	Re-oxidation	[42]
Phosphorus	Precipitation, sorption	Vivianite, ferrihydrite	Release under reducing conditions	[14, 15]
Organics, pharmaceuticals	Radical oxidation	Fe(II)/Fe(III) with H2O2 or persulfate	Sludge, iron leaching	[28, 53, 70–73, 75, 101]

Table 5 shows that contaminant chemistry determines both the mechanism and the main failure mode. Redox-sensitive species (Cr(VI), U, chlorinated solvents, and nitrate) are removed by electron transfer and are vulnerable to re-oxidation or passivation, whereas oxyanions (As and P) are removed by sorption and co-precipitation and are vulnerable to release during recrystallization or reductive dissolution [1, 13–15, 20, 34, 40–42, 49, 51, 54, 84–88].

Figure 3. Qualitative suitability of iron-based approaches by contaminant class. Scores (none, low, moderate, high) are assigned by the author from the performance and mechanism evidence in Tables 4 and 5 and refs [13–15, 20, 21, 28, 34, 38, 39, 42, 49, 51, 53, 54, 70, 71, 84–88]; they are a synthesis aid, not measured values.

Figure 3 combines the mechanisms in Table 5 with the performance in Table 4. High suitability follows mechanism: ZVI-based routes for Cr(VI) and chlorinated solvents [20, 21, 28, 54, 84–86], iron oxides and biogenic minerals for arsenic and uranium [13–15, 42, 51, 87, 88], Fe-cycling bioreactors and vivianite for nitrate and phosphorus [13–15, 49, 51, 88], and Fenton systems only for organics [28, 53, 70, 71]. The pattern is one of specialization, which is why no single iron technology can serve all sites and why the decision framework (Table 8) starts from the contaminant and the redox regime.

4.3 Environmental controls on performance

Environmental conditions modulate every route (Table 6). pH determines Fe(II) solubility and oxide formation and therefore sets the optimum for biogenic versus Fenton-type routes [1, 28, 40, 41, 53, 70, 71]. Organic carbon and electron shuttles accelerate microbial reduction and contaminant transformation but may also mobilize metals [45]. Sulfide alters ZVI selectivity [20, 21, 28], while oxygen and nitrate drive Fe(II) oxidation, which re-immobilizes arsenic and phosphorus [2, 49–51]. Mineral crystallinity, which evolves with time, governs reactivity and trace-metal retention, so aging reduces capacity in long-term installations [1, 38–41, 54]. Figure 4 summarizes the reported decline in ZVI reactivity under oxic aging compared with anoxic or sulfidated conditions [19–21, 28, 34, 38, 39, 49, 54, 84–86].

Table 6
Influence of environmental variables on iron-based remediation performance.

Variable	Effect on Fe(II)/Fe(III) cycling	Consequence for remediation	Refs
pH	Controls Fe(II) solubility and oxide formation	Optimum near neutral for most biogenic routes; acidic for Fenton	[1, 28, 40, 41, 53, 70, 71]
Organic carbon / electron shuttles	Accelerates microbial reduction	Faster contaminant transformation, risk of mobilization	[45]
Sulfate and sulfide	Forms FeS, passivates or activates ZVI	Selectivity shifts toward sulfidic pathways	[20, 21, 28]
Oxygen and nitrate	Drives Fe(II) oxidation	Re-immobilization of As and P; N2O risk	[2, 49–51]
Mineral crystallinity	Controls reactivity and trace-metal retention	Aging reduces capacity over time	[1, 38–41, 54, 58, 61]

Table 6 identifies the parameters that link the results. pH sets Fe(II) solubility and the optimum for biogenic versus Fenton routes; sulfide and organic carbon steer selectivity and microbial rates; oxygen and nitrate drive re-oxidation; and crystallinity, which evolves with time, governs reactivity and trace-metal retention [1, 2, 20, 21, 28, 38–41, 45, 49–51, 53, 54, 70, 71]. These variables explain the spread in Table 4 and the aging trend in Fig. 4.

Figure 4 links aging to the controls in Table 6. Oxic conditions drive oxide-shell growth and the fastest loss of ZVI reactivity, anoxic conditions slow it, and sulfidation delays it further by altering surface sites [19–21, 28, 34, 54]. The trend implies that pH, oxygen, sulfide, and mineral crystallinity jointly determine the service life of PRBs and injected iron [38, 39, 54, 58, 61]. In practice, passivation therefore appears as declining removal efficiency and rising maintenance demand.

4.4 Sustainability indicators

Green chemistry indicators favor plant-extract nZVI, biogenic minerals, and slag- or sludge-derived iron over borohydride-synthesized nZVI and homogeneous Fenton systems (Table 7, Fig. 5). Plant-extract routes avoid hazardous reductants and lower synthesis energy [31, 34]. Biogenic phases combine very low reagent hazard with the potential to recover iron and phosphorus [13–15, 42, 51, 87, 88]. Waste-derived iron lowers embodied impacts and supports circularity [36, 37], and life-cycle and techno-economic studies indicate that these advantages depend on transport distance, dosing, and replacement frequency [102, 103]. Homogeneous Fenton chemistry scores poorly mainly because of sludge generation [28, 53, 70, 71].

Table 7
Green-chemistry and sustainability indicators for selected iron-based routes.

Route	Reagent hazard	Energy demand	Waste/sludge	Circularity potential	Refs
Borohydride nZVI	High	Medium	Medium	Low	[19, 20, 34, 49, 54, 84–86]
Plant-extract nZVI	Low	Low	Low	Medium	[31, 34]
Biogenic minerals	Very low	Low	Low	High (P, Fe recovery)	[13–15, 42, 51, 87, 88]
Fenton (homogeneous)	Medium	Low	High	Low	[28, 53, 70, 71]
Slag/sludge-derived Fe	Low	Low	Low	High	[36, 37, 83, 102, 103]

Table 7 shows that reagent hazard, energy demand, waste, and circularity do not vary together. Plant-extract nZVI lowers hazard but improves circularity only moderately, biogenic minerals and slag- or sludge-derived iron score favorably on all four indicators, and homogeneous Fenton is penalized mainly by sludge [13–15, 28, 31, 34, 36, 37, 42, 51, 53, 70, 71, 87, 88, 102, 103].

Figure 5 shows that biogenic minerals and slag- or sludge-derived iron score highest on the four indicators, plant-extract nZVI is intermediate, and borohydride nZVI and homogeneous Fenton score lowest because of reagent hazard and sludge [13–15, 28, 31, 34, 36, 37, 42, 51, 53, 70, 71, 87, 88, 102, 103]. Combined with Table 4, this reveals a trade-off: the most sustainable biogenic routes tend to be slower and more site-dependent, whereas high-rate chemical routes carry higher reagent and waste burdens [13, 49, 51, 88, 102, 103].

5. Discussion

5.1 Mineral transformation governs durability

Across all approaches, the persistence of removal depends on what happens to the iron phase after the contaminant has been captured. Fe(II)-catalyzed recrystallization and atom exchange can convert poorly crystalline oxides into more ordered phases over hours to months, and during this transformation, co-precipitated elements such as arsenic may be incorporated into the structure or released to solution, depending on pH and Fe(II) supply [1, 40, 41]. In ZVI systems, oxide-shell growth and the accumulation of corrosion products passivate the surface, and sulfidation changes both the initial reactivity and the aging pathway [19–21, 28, 34, 38, 39, 54]. In biogenic systems, durability depends on whether reducing conditions persist, because oxidation of Fe(II) minerals can re-release immobilized contaminants [2, 13–15, 42, 49–51, 87, 88].

Three design consequences follow. First, systems that pair a reductive phase with a sorptive phase, or that regenerate reactive Fe(II) through microbial reduction, are less exposed to a single failure mode [13–15, 42, 49, 51, 87, 88]. Second, performance should be evaluated over aging cycles and not only at the start of an experiment [35, 38, 39, 54]. Third, the stabilizing conditions (pH, sulfide, carbonate, and carbon supply) should be treated as design variables linked to the target mineral phase (Tables 1, 5, and 6) [1, 13–15, 20, 21, 28, 40–42, 51, 87, 88].

5.2 Integrating microbial and abiotic processes

Biogenic and bio-inspired routes improve green metrics but depend on conditions that are harder to control than those in a chemical reactor. Iron-reducing communities respond to electron-donor supply, electron shuttles, and competition from nitrate and sulfate [43–45], and Fe(II)-oxidizing processes can reverse removal if oxygen or nitrate intrudes [2, 49–51]. Abiotic reactive media provide fast and predictable kinetics but lack self-regeneration. Hybrid designs aim to combine these properties: microbial reduction can regenerate Fe(II) at ZVI or mineral surfaces, and electrodes can impose a redox potential that stabilizes the microbial community regardless of season [13, 44, 45, 49, 51, 88–90]. Such integration is plausible on the basis of the cited work, but few studies appear to have tested it over long periods, which is a key gap (Table 9) [13, 44, 45, 49, 51, 88–90].

5.3 Risks and greenhouse-gas by-products

Iron-based systems can produce unintended outcomes that must be weighed against their benefits. Fe(II)-driven denitrification can generate nitrite and N_2O, a potent greenhouse gas, when denitrification is incomplete [2, 49–51]. Iron-mediated processes can suppress methane in some soils and sediments but may stimulate it in others, depending on the balance between iron reducers and methanogens [12]. Release of arsenic or phosphorus during reductive dissolution of Fe(III) oxides is the main secondary water-quality risk in biogenic and wetland systems [1, 9, 14, 15, 40, 41]. Nanoscale iron raises additional questions of mobility and ecotoxicity [19, 104]. These risks argue for monitoring gases and speciation during pilots and for including by-products in the performance criteria [19, 35, 38, 39].

5.4 Scale-up and field evidence

Most evidence derives from batch or column experiments with synthetic or lightly amended waters, and standardized reporting of dose, iron speciation, aging, and hydraulics is rare [19, 35, 38, 39]. Natural organic matter, carbonate, sulfate, and co-contaminants alter surface reactivity and microbial activity, so laboratory removal ranges (Table 4, Fig. 2) tend to overstate field performance [19, 20, 34, 35, 39, 49, 54, 84–86]. Field deployments of PRBs and injected iron identify clogging, flow bypass, and loss of reactivity as the main failure modes [38, 39, 54], and cost and regulatory acceptance add further constraints for novel materials [35, 38]. A staged path from batch tests, through column studies with real water, to pilot injection or barrier trials with mineralogical tracking would narrow this gap [38, 39, 54].

5.5 Circularity and life-cycle perspective

Using slag, mine-drainage sludge, and water-treatment residuals as iron sources can reduce embodied impacts and align remediation with circular economy goals [36, 37]. Life-cycle and techno-economic studies show that the benefits are sensitive to logistics, activation energy, and replacement frequency [102, 103]. A material that is sustainable to synthesize may still be unsustainable if frequent replacement is needed because of passivation. This links the sustainability results (Table 7, Fig. 5) to the durability results (Table 6, Fig. 4) [19, 34, 38, 39, 54, 102, 103]. Comparative life-cycle assessment should therefore accompany the development of new materials.

5.6 Positioning relative to other remediation options

Iron-based routes complement rather than replace other options. Sorbents and membranes remove contaminants without transforming them, whereas iron-based reduction and oxidation can destroy or immobilize redox-active species [35, 36, 39]. Compared with conventional chemical oxidation and pump-and-treat, iron-cycle approaches can lower reagent and energy demand but depend more strongly on site mineralogy and redox conditions [28, 35, 38, 39, 53, 54, 70, 71]. Iron-cycle strategies are therefore most advantageous where redox-active contaminants, existing iron minerals, and long treatment horizons coincide, as reflected in the decision framework below.

5.7 Decision framework

Combining the mechanisms (Table 5), environmental controls (Table 6), and sustainability indicators (Table 7), Table 8 and Fig. 6 outline a site-based decision process that maps the dominant contaminant and redox setting to a strategy and a monitoring priority [1, 13–15, 20, 21, 28, 36–42, 49, 51, 53, 54, 70, 71, 87, 88, 102, 103].

Table 8
Decision framework for selecting an iron-cycle-based strategy.

Site condition	Dominant contaminant	Recommended strategy	Monitoring priority	Refs
Anoxic aquifer, circumneutral pH	Cr(VI), chlorinated solvents	Sulfidated ZVI PRB or colloid injection	Hydraulics, Fe speciation	[20, 21, 28, 38, 39, 54]
Redox-fluctuating floodplain	As, P	Biogenic Fe(III) oxide management, wetland cycling	Eh, Fe(II)/Fe(III), As speciation	[1, 13–15, 40, 41, 49, 51, 88]
Acid mine drainage	Metals, sulfate	Circular Fe sludge plus biological neutralization	pH, sludge stability	[36, 37, 83]
Industrial wastewater	Organics, dyes	Heterogeneous Fenton on waste-derived supports	Oxidant dose, leaching	[28, 53, 70, 71]

Table 8 condenses the results into rules of thumb: the redox regime and dominant contaminant (Tables 2 and 5) select the strategy, and the monitoring priority follows from the main failure mode identified in Tables 5 and 6 [1, 13–15, 20, 21, 28, 36–41, 49, 51, 53, 54, 70, 71, 88].

Figure 6 turns these results into a sequence. Site characterization (contaminant, pH, Eh, and Fe speciation) identifies the redox regime, which selects the route in Table 8: ZVI barriers in stable anoxic settings, biogenic and wetland cycling where redox conditions fluctuate, and Fenton chemistry for oxidizable organics [13, 20, 21, 28, 38, 39, 49, 51, 53, 54, 70, 71, 88]. Circular iron sourcing and the monitoring of hydraulics, speciation, and by-products apply to all branches [2, 12, 36, 37, 50, 51, 102, 103].

5.8 Research priorities

The limitations identified above lead to the priorities summarized in Table 9: long-duration field trials, standardized reporting, by-product control, circular sourcing, control of mineral aging, and predictive models that link geochemical descriptors to outcomes [19, 35–39, 54, 102, 103, 105].

Table 9
Research priorities and proposed approaches.

Priority	Knowledge gap	Proposed approach	Refs
Long-duration field trials	Aging, clogging, loss of reactivity	Multi-year pilots with mineralogical tracking	[35, 38, 39, 54]
Standardized reporting	Dose, speciation, matrix not reported	Shared reporting checklist for iron systems	[19, 35, 38, 39]
By-product control	N2O and CH4 formation	Monitor gases; tune electron donors and oxidants	[2, 12, 50, 51]
Circular sourcing	Variable composition of waste iron	Life-cycle and techno-economic assessment	[36, 37, 102, 103]
Mineral-aging control	Release during recrystallization	Phase stabilization; paired sorptive and reductive phases	[1, 20, 21, 28, 40, 41]
Predictive models	Weak link from geochemistry to outcomes	Machine learning on geochemical descriptors	[105]

Table 9 links each priority to a gap identified in the preceding sections: aging and clogging (Table 6, Fig. 4), missing field data (Table 4), by-products (Table 2), and circular sourcing (Table 7, Fig. 5) [19, 35–39, 54, 102, 103].

5.9 Limitations of the evidence

Reported removal ranges depend on initial concentrations, water matrices, and experimental design, which limits direct comparison [19, 35, 38, 39]. Many studies lack aging experiments, real-water matrices, and by-product measurements, and publication bias toward positive results is likely [19, 20, 34, 35, 39, 49, 54, 84–86]. The figures and tables in this review (Figs. 2–5 and Tables 4 and 7) are syntheses of reported trends and qualitative ratings, not meta-analyses. Shared reporting standards and quantitative meta-analysis would improve future comparisons.

6. Conclusions

The biogeochemical iron cycle provides both the mechanistic basis and the material supply for low-impact remediation. The evidence reviewed here indicates that green-synthesized and biogenic iron phases can approach the performance of conventional iron-based treatments for arsenic, chromium, nitrate, and chlorinated solvents while reducing reagent hazard and energy use. Performance and durability are governed by a small set of linked parameters: pH, redox potential, sulfide and carbon availability, oxygen and nitrate intrusion, and the crystallinity of iron minerals. Because these parameters vary between sites, no single technology is suitable everywhere, and technology selection should begin with the dominant contaminant and the redox regime of the site.

The main weaknesses of the current literature are the scarcity of long-term and field-scale data, inconsistent reporting of dose, speciation, and aging, and the limited quantitative assessment of

sustainability. Addressing them will require multi-year pilots with mineralogical tracking, standardized reporting, assessment of nitrous oxide and methane by-products, circular iron sourcing supported by life-cycle analysis, and models that connect geochemical descriptors to remediation outcomes. Progress on these points would move iron-cycle-informed remediation from promising laboratory results to dependable, low-carbon, geoscience-based practice.

Declarations

Clinical trial number

Not applicable.

Ethics approval and consent to participate:

Not applicable.

Consent for publication:

Not applicable.

Competing interests:

The authors declare no competing interests.

Third-party material

Not applicable.

Funding:

The authors received no specific funding for this work.

Author Contribution

D. J. Methodology, Investigation, Formal analysis, Data curation, Writing – original draft. R.S. Conceptualization, Methodology, Supervision, Validation, Writing – review & editing, Project administration. S.S. Validation, Visualization, Formal analysis.

Data availability:

Not applicable.

References

1. Huang J, Jones A, Waite TD, Chen Y, Huang X, Rosso KM, Kappler A, Mansor M, Tratnyek PG, Zhang H. Fe(II) redox chemistry in the environment. Chem Rev. 2021;121:8161–233. https://doi.org/10.1021/acs.chemrev.0c01286.
2. Kappler A, Bryce C, Mansor M, Lueder U, Byrne JM, Swanner ED. An evolving view on biogeochemical cycling of iron. Nat Rev Microbiol. 2021;19:360–74. https://doi.org/10.1038/s41579-020-00502-7.
3. Yan L, Li S, Sivan O, Kasten S. Editorial: Advances in microbial iron cycling. Front Microbiol. 2022;13:931648. https://doi.org/10.3389/fmicb.2022.931648.
4. Song X, Wang P, Van Zwieten L, Bolan N, Wang H, Li X, Cheng K, Yang Y, Wang M, Liu T, Li F. Towards a better understanding of the role of Fe cycling in soil for carbon stabilization and degradation. Carbon Res. 2022;1:5. https://doi.org/10.1007/s44246-022-00008-2.
5. Dong H, Zeng Q, Sheng Y, Chen C, Yu G, Kappler A. Coupled iron cycling and organic matter transformation across redox interfaces. Nat Rev Earth Environ. 2023;4:659–73. https://doi.org/10.1038/s43017-023-00470-5.
6. Kleber M, Bourg IC, Coward EK, et al. Dynamic interactions at the mineral–organic matter interface. Nat Rev Earth Environ. 2021;2:402–21. https://doi.org/10.1038/s43017-021-00162-y.
7. Jia N, Li L, Guo H, et al. Important role of Fe oxides in global soil carbon stabilization and stocks. Nat Commun. 2024;15:10318. https://doi.org/10.1038/s41467-024-54832-8.
8. Ni B, Yu X, Duan X, Zou Y. Wetland soil organic carbon balance is reversed by old carbon and iron oxide additions. Front Microbiol. 2024;14:1327265. https://doi.org/10.3389/fmicb.2023.1327265.
9. Bao Y, Bolan NS, Lai J, Wang Y, Jin X, Kirkham MB, Wu X, Fang Z, Zhang Y, Wang H. Interactions between organic matter and Fe (hydr)oxides and their influences on immobilization and remobilization of metal(loid)s: a review. Crit Rev Environ Sci Technol. 2022;52:4016–37. https://doi.org/10.1080/10643389.2021.1974766.
10. Moore OC, et al. The role of electron donors in arsenic-release by redox-transformation of iron oxide minerals: a review. Chem Geol. 2023;619:121322. https://doi.org/10.1016/j.chemgeo.2023.121322.
11. Patzner MS, Logan M, McKenna AM, Young RB, Zhou Z, Joss H, Mueller CW, Hoeschen C, Scholten T, Straub D, Kleindienst S, Borch T, Kappler A, Bryce C. Microbial iron cycling during palsa hillslope collapse promotes greenhouse gas emissions before complete permafrost thaw. Commun Earth Environ. 2022;3:76. https://doi.org/10.1038/s43247-022-00407-8.
12. Cai C, Ni G, Xia J, Zhang X, Zheng Y, He B, Marcellin E, Li W, Pu J, Yuan Z, Hu S. Response of the anaerobic methanotrophic archaeon Candidatus Methanoperedens nitroreducens to the long-term ferrihydrite amendment. Front Microbiol. 2022;13:799859. https://doi.org/10.3389/fmicb.2022.799859.

13. Darma A, Yang J, Bloem E, Możdżen K, Zandi P. Arsenic biotransformation and mobilization: the role of bacterial strains and other environmental variables. Environ Sci Pollut Res. 2022;29:1763–87. https://doi.org/10.1007/s11356-021-17117-x.
14. Zhang J, Chen Z, Liu Y, Wei W, Ni BJ. Phosphorus recovery from wastewater and sewage sludge as vivianite. J Clean Prod. 2022;370:133439. https://doi.org/10.1016/j.jclepro.2022.133439.
15. Aguilar-Pozo VB, Tamayo P, Casallas-Ojeda M, Siscar E, Fonoll X, Chimenos JM, Astals S. Phosphorus recovery via vivianite precipitation in anaerobic digestion and fermentation processes: a comprehensive review. Sustain Chem Pharm. 2025;48. https://doi.org/10.1016/j.scp.2025.102237.
16. Wang CC, Zhang QC, Yan CA, Tang GY, Zhang MY, Ma LQ, Gu RH, Xiang P. Heavy metal(loid)s in agriculture soils, rice, and wheat across China: status assessment and spatiotemporal analysis. Sci Total Environ. 2023;882:163361. https://doi.org/10.1016/j.scitotenv.2023.163361.
17. Song P, Xu D, Yue J, Ma Y, Dong S, Feng J. Recent advances in soil remediation technology for heavy metal contaminated sites: a critical review. Sci Total Environ. 2022;838:156417. https://doi.org/10.1016/j.scitotenv.2022.156417.
18. Rajendran S, Priya TAK, Khoo KS, Hoang TKA, Ng HS, Munawaroh HSH, Karaman C, Orooji Y, Show PL. A critical review on various remediation approaches for heavy metal contaminants removal from contaminated soils. Chemosphere. 2022;287:132369. https://doi.org/10.1016/j.chemosphere.2021.132369.
19. Alazaiza MYD, Albahnasawi A, Copty NK, Bashir MJK, Nassani DE, Al Maskari T, Abu Amr SS, Abujazar MSS. Nanoscale zero-valent iron application for the treatment of soil, wastewater and groundwater contaminated with heavy metals: a review. Desalin Water Treat. 2022;253:194–210. https://doi.org/10.5004/dwt.2022.28302.
20. Garcia AN, Zhang Y, Ghoshal S, He F, O'Carroll DM. Recent Advances in Sulfidated Zerovalent Iron for Contaminant Transformation. Environ Sci Technol. 2021;55(13):8464–83. 10.1021/acs.est.1c01251.
21. Xue W, Li J, Chen X, Liu H, Wen S, Shi X, Guo J, Gao Y, Xu J, Xu Y. Recent advances in sulfidized nanoscale zero-valent iron materials for environmental remediation and challenges. Environ Sci Pollut Res. 2023;30:101933–62. https://doi.org/10.1007/s11356-023-29564-9.
22. Li F, Wang X, Xu C. Research progress on structural characteristics, structure–application relationships, and environmental application of biochar-supported zero valent iron (ZVI-BC). Curr Pollut Rep. 2023;9:292–311. https://doi.org/10.1007/s40726-023-00260-z.
23. Zhong X, Lai Y, Wang X, Wang M, Han W, Zhang M, Ji H. Synthesis and environmental applications of biochar-supported nano-zero-valent iron composites: a review. Environ Chem Lett. 2024;22:1345–63. https://doi.org/10.1007/s10311-024-01712-8.
24. Awang NA, Salleh W, Aziz WN, Yusof F, N. and, Ismail AF. A review on preparation, surface enhancement and adsorption mechanism of biochar-supported nano zero-valent iron adsorbent for

hazardous heavy metals. J Chem Technol Biotechnol. 2023;98:22–44. https://doi.org/10.1002/jctb.7182.

25. Tang H, Wang J, Zhang S, Pang H, Wang X, Chen Z, Li M, Song G, Qiu M, Yu S. Recent advances in nanoscale zero-valent iron-based materials: characteristics, environmental remediation and challenges. J Clean Prod. 2021;319:128641. https://doi.org/10.1016/j.jclepro.2021.128641.
26. Wang P, Fu F, Liu T. A review of the new multifunctional nano zero-valent iron composites for wastewater treatment: emergence, preparation, optimization and mechanism. Chemosphere. 2021;285:131435. https://doi.org/10.1016/j.chemosphere.2021.131435.
27. Liang W, Wang G, Peng C, Tan J, Wan J, Sun P, Li Q, Ji X, Zhang Q, Wu Y, et al. Recent advances of carbon-based nano zero valent iron for heavy metals remediation in soil and water: a critical review. J Hazard Mater. 2022;426:127993. https://doi.org/10.1016/j.jhazmat.2021.127993.
28. Sun Y, Liu J, Fan X, Li Y, Peng W. Synthesis and application of iron sulfide-based materials to activate persulfates for wastewater remediation: a review. Front Environ Sci. 2023;11:1212355. https://doi.org/10.3389/fenvs.2023.1212355.
29. Fan XD, Lin QT, Zheng JL, Fu HY, Xu KH, Liu YX, Ma YJ, He J. Peroxydisulfate activation by nano zero-valent iron graphitized carbon materials for ciprofloxacin removal: effects and mechanism. J Hazard Mater. 2022;437:129392. https://doi.org/10.1016/j.jhazmat.2022.129392.
30. Castiello C, Junghanns P, Mergel A, Jacob C, Ducho C, Valente S, Rotili D, Fioravanti R, Zwergel C, Mai A. GreenMedChem: the challenge in the next decade toward eco-friendly compounds and processes in drug design. Green Chem. 2023;25:2109–69. https://doi.org/10.1039/D2GC03772F.
31. Kheskwani U, Ahammed MM. Removal of water pollutants using plant-based nanoscale zero-valent iron: a review. Water Sci Technol. 2023;88:1207–31. https://doi.org/10.2166/wst.2023.270.
32. Han X, Zhao Y, Zhao F, Wang F, Tian G, Liang J. Novel synthesis of nanoscale zero-valent iron from iron ore tailings and green tea for the removal of methylene blue. Colloids Surf A. 2023;656:130412. https://doi.org/10.1016/j.colsurfa.2022.130412.
33. Slijepcevic N, Pilipovic DT, Kerkez D, Krcmar D, Becelic-Tomin M, Beljin J, Dalmacija B. A cost effective method for immobilization of Cu and Ni polluted river sediment with nZVI synthesized from leaf extract. Chemosphere. 2021;263:127816. https://doi.org/10.1016/j.chemosphere.2020.127816.
34. Teng W, Yang K, Chen J, Li H, Han J. Application and mechanism of various modified nano zero-valent iron in wastewater treatment: a critical review. Green Chem. 2025;27:10045–70. https://doi.org/10.1039/D5GC02077H.
35. Sheikh MS, Kolo K, Hamad SM. Synergetic interactions of nanoscale zero-valent iron (nZVI) and anaerobic bacteria in groundwater remediation: a review. Eurasian J Sci Eng. 2022;8:35–53.
36. O'Connor J, Nguyen TBT, Honeyands T, Monaghan B, O'Dea D, Rinklebe J, Vinu A, Hoang SA, Singh G, Kirkham MB, Bolan N. Production, characterisation, utilisation, and beneficial soil application of steel slag: a review. J Hazard Mater. 2021;419:126478. https://doi.org/10.1016/j.jhazmat.2021.126478.
37. Chowdhury SR. Recycled smelter slags for in situ and ex situ water and wastewater treatment: current knowledge and opportunities. Processes. 2023;11:783.

https://doi.org/10.3390/pr11030783.

38. Lawrinenko M, Kurwadkar S, Wilkin RT. Long-term performance evaluation of zero-valent iron amended permeable reactive barriers for groundwater remediation – a mechanistic approach. Geosci Front. 2023;14:101494. https://doi.org/10.1016/j.gsf.2022.101494.
39. Bilardi S, Calabrò PS, Moraci N. A review of the hydraulic performance of permeable reactive barriers based on granular zero valent iron. Water. 2023;15:200. https://doi.org/10.3390/w15010200.
40. Schulz K, ThomasArrigo LK, Kaegi R, Kretzschmar R. Stabilization of ferrihydrite and lepidocrocite by silicate during Fe(II)-catalyzed mineral transformation: impact on particle morphology and silicate distribution. Environ Sci Technol. 2022;56:5929–38. https://doi.org/10.1021/acs.est.1c08789.
41. Perez JPH, Tobler DJ, Freeman HM, Brown AP, Hondow NS, van Genuchten CM, Benning LG. Arsenic species delay structural ordering during green rust sulfate crystallization from ferrihydrite. Environ Sci Nano. 2021;8:2950–63. https://doi.org/10.1039/d1en00384d.
42. Matulová M, Duborská E, Matúš P, Urík M. Solid–water interface interaction of selenium with Fe(II)-bearing minerals and aqueous Fe(II) and S(-II) ions in the near-field of the radioactive waste disposal system. Int J Mol Sci. 2023;24:315. https://doi.org/10.3390/ijms24010315.
43. Gralnick JA, Bond DR. Electron transfer beyond the outer membrane: putting electrons to rest. Annu Rev Microbiol. 2023;77:517–39. (add DOI).
44. Zou L, Zhu F, Long ZE, Huang Y. Bacterial extracellular electron transfer: a powerful route to the green biosynthesis of inorganic nanomaterials for multifunctional applications. J Nanobiotechnol. 2021;19:120. https://doi.org/10.1186/s12951-021-00868-7.
45. Zang Y, Cao B, Zhao H, Xie B, Ge Y, Liu H, Yi Y. Mechanism and applications of bidirectional extracellular electron transfer of Shewanella. Environ Sci Process Impacts. 2023;25:1863–77. https://doi.org/10.1039/D3EM00224A.
46. Peiffer S, Kappler A, Haderlein SB, Schmidt C, Byrne JM, et al. A biogeochemical–hydrological framework for the role of redox-active compounds in aquatic systems. Nat Geosci. 2021;14:264–72. https://doi.org/10.1038/s41561-021-00742-z. (check full author list).
47. Abuyen K, El-Naggar MY. Soluble iron enhances extracellular electron uptake by Shewanella oneidensis MR-1. ChemElectroChem. 2023;10:e202200965. https://doi.org/10.1002/celc.202200965.
48. Liang D, Liu X, Woodard TL, Holmes DE, Smith JA, Nevin KP, et al. Extracellular electron exchange capabilities of Desulfovibrio ferrophilus and Desulfopila corrodens. Environ Sci Technol. 2021;55:16195–203. https://doi.org/10.1021/acs.est.1c04071.
49. Pang S, Li N, Luo H, Luo X, Shen T, Yang Y, Jiang J. Autotrophic Fe-driven biological nitrogen removal technologies for sustainable wastewater treatment. Front Microbiol. 2022;13:895409. https://doi.org/10.3389/fmicb.2022.895409.
50. Visser AN, Wankel SD, Frey C, Kappler A, Lehmann MF. Unchanged nitrate and nitrite isotope fractionation during heterotrophic and Fe(II)-mixotrophic denitrification suggest a non-enzymatic

link between denitrification and Fe(II) oxidation. Front Microbiol. 2022;13:927475. https://doi.org/10.3389/fmicb.2022.927475.

51. Koepnick HR, Peyton BM, Lauchnor EG. Nitrate-dependent iron oxidation for bioremediation of metal, metalloid, and radionuclide contaminants. Rev Environ Sci Biotechnol. 2025;24:661–94. https://doi.org/10.1007/s11157-025-09736-4.
52. Zhou N, Kupper RJ, Catalano JG, Thompson A, Chan CS. Biological oxidation of Fe(II)-bearing smectite by microaerophilic iron oxidizer Sideroxydans lithotrophicus using dual Mto and Cyc2 iron oxidation pathways. Environ Sci Technol. 2022;56:17443–53. https://doi.org/10.1021/acs.est.2c05142.
53. Sun W, Wang S, Yu Z, Cao X. Characteristics and application of iron-based materials in heterogeneous Fenton oxidation for wastewater treatment: a review. Environ Sci Water Res Technol. 2023;9:1266–89. https://doi.org/10.1039/D2EW00810F.
54. Plessl K, Russ A, Vollprecht D. Application and development of zero-valent iron (ZVI) for groundwater and wastewater treatment. Int J Environ Sci Technol. 2023;20:6913–28. https://doi.org/10.1007/s13762-022-04536-7.
55. Huang Q, Gu T, Liu A, Liu J, Zhang W. Probing pollutant reactions at the iron surface: a case study on selenite reactions with nanoscale zero-valent iron. Environ Sci Nano. 2021;8:2650–9. https://doi.org/10.1039/D1EN00458A.
56. Prasad S, Yadav KK, Kumar S, Gupta N, Cabral-Pinto MMS, Rezania S, Radwan N, Alam J. Chromium contamination and effect on environmental health and its remediation: a sustainable approaches. J Environ Manage. 2021;285:112174. https://doi.org/10.1016/j.jenvman.2021.112174.
57. Izadi N, Ali BH, Shahin MS, Baghdadi M. The removal of Cr(VI) from aqueous and saturated porous media by nanoscale zero-valent iron stabilized with flaxseed gum extract: synthesis by continuous flow injection method. Korean J Chem Eng. 2022;39:2217–28. https://doi.org/10.1007/s11814-022-1069-4.
58. Li X, Gao M, Huo Y, Liu H, Li J, Huang T, Ye R, Li W. Impacts of shell structure on nitrate-reduction activity and air stability of nanoscale zero-valent iron. Environ Sci Pollut Res. 2022;29:80683–92. https://doi.org/10.1007/s11356-022-21460-y.
59. Maamoun I, Falyouna O, Eljamal R, Bensaida K, Tanaka K, Tosco T, Sugihara Y, Eljamal O. Multi-functional magnesium hydroxide coating for iron nanoparticles towards prolonged reactivity in Cr(VI) removal from aqueous solutions. J Environ Chem Eng. 2022;10:107431. https://doi.org/10.1016/j.jece.2022.107431.
60. Wang P, Hu J, Liu T, Han G, Ma WM, Li J. New insights into ball-milled zero-valent iron composites for pollution remediation: an overview. J Clean Prod. 2023;385:135513. https://doi.org/10.1016/j.jclepro.2022.135513.
61. Hu YB, Ma L, Yuan B, Li XY. Confining polyacrylic acid on the surface of nanoscale zero-valent iron by aluminum hydroxide for in-situ anti-passivation. J Hazard Mater. 2021;420:126649. https://doi.org/10.1016/j.jhazmat.2021.126649.

62. Tian H, Huang C, Wang P, Wei J, Li X, Zhang R, Ling D, Feng C, Liu H, Wang M, et al. Enhanced elimination of Cr(VI) from aqueous media by polyethyleneimine modified corn straw biochar supported sulfide nanoscale zero valent iron: performance and mechanism. Bioresour Technol. 2023;369:128452. https://doi.org/10.1016/j.biortech.2022.128452.
63. Zhou G, Chen JQ, He CS, Ding R, Mu Y. Nano-sized zero-valent iron coupled with sulfidation and ferrous implantation enhances the reduction–oxidation removal of iodinated contrast medium. ACS EST Water. 2021;1:2128–38. https://doi.org/10.1021/acsestwater.1c00199.
64. Shen W, Xu J, Zhu L. Triton X-100 improves the reactivity and selectivity of sulfidized nanoscale zerovalent iron toward tetrabromobisphenol A: implications for groundwater and soil remediation. J Hazard Mater. 2021;416:126119. https://doi.org/10.1016/j.jhazmat.2021.126119.
65. He Y, Fang T, Wang J, Liu X, Yan Z, Lin H, Li F, Guo G. Insight into the stabilization mechanism and long-term effect on As, Cd, and Pb in soil using zeolite-supported nanoscale zero-valent iron. J Clean Prod. 2022;355:131634. https://doi.org/10.1016/j.jclepro.2022.131634.
66. Falyouna O, Maamoun I, Bensaida K, Tahara A, Sugihara Y, Eljamal O. Encapsulation of iron nanoparticles with magnesium hydroxide shell for remarkable removal of ciprofloxacin from contaminated water. J Colloid Interface Sci. 2022;605:813–27. https://doi.org/10.1016/j.jcis.2021.07.154.
67. Falyouna O, Maamoun I, Bensaida K, Tahara A, Sugihara Y, Eljamal O. Chemical deposition of iron nanoparticles (Fe0) on titanium nanowires for efficient adsorption of ciprofloxacin from water. Water Pract Technol. 2022;17:75–83. https://doi.org/10.2166/wpt.2021.091.
68. Li S, Li C, Gao X, Zhu M, Li H, Wang X. Biomineralization mediated by iron-oxidizing microorganisms: implication for the immobilization and transformation of heavy metals in AMD. Minerals. 2025;15:868. https://doi.org/10.3390/min15080868.
69. Shi J, Wu X, Zhao X, Zhou J, Liu S, Li B, Zhang J, Li W, Zeng X, Wang X, et al. Remediation of heavy metal-contaminated estuarine sediments by strengthening microbial in-situ mineralization. Appl Geochem. 2024;169:106051. https://doi.org/10.1016/j.apgeochem.2024.106051.
70. Yao Y, Pan Y, Yu Y, Yu Z, Lai L, Liu F, Wei L, Chen Y. Bifunctional catalysts for heterogeneous electro-Fenton processes: a review. Environ Chem Lett. 2022;20:3837–59. https://doi.org/10.1007/s10311-022-01453-6.
71. Wang Z, Liu M, Xiao F, Postole G, Zhao H, Zhao G. Recent advances and trends of heterogeneous electro-Fenton process for wastewater treatment: review. Chin Chem Lett. 2022;33:653–62. https://doi.org/10.1016/j.cclet.2021.07.044.
72. Hussain S, Aneggi E, Goi D. Catalytic activity of metals in heterogeneous Fenton-like oxidation of wastewater contaminants: a review. Environ Chem Lett. 2021;19:2405–24. https://doi.org/10.1007/s10311-021-01185-z.
73. Liu Y, Zhao Y, Wang J. Fenton/Fenton-like processes with in-situ production of hydrogen peroxide/hydroxyl radical for degradation of emerging contaminants: advances and prospects. J Hazard Mater. 2021;404:124191. https://doi.org/10.1016/j.jhazmat.2020.124191.

74. Shang Y, Xu X, Gao B, Wang S, Duan X. Single-atom catalysis in advanced oxidation processes for environmental remediation. Chem Soc Rev. 2021;50:5281–322. https://doi.org/10.1039/D0CS01032D.
75. Yan Q, Lian C, Huang K, Liang L, Yu H, Yin P, Zhang J, Xing M. Constructing an acidic microenvironment by MoS2 in heterogeneous Fenton reaction for pollutant control. Angew Chem Int Ed. 2021;60:17155–63. https://doi.org/10.1002/anie.202105736.
76. Liu Z, Wan J, Ma Y, Wang Y. In situ synthesis of FeOCl@MoS2 on graphite felt as novel electro-Fenton cathode for efficient degradation of antibiotic ciprofloxacin at mild pH. Chemosphere. 2021;273:129747. https://doi.org/10.1016/j.chemosphere.2021.129747.
77. Liang J, Xiang Q, Lei W, Zhang Y, Sun J, Zhu H, Wang S. Ferric iron reduction reaction electro-Fenton with gas diffusion device: a novel strategy for improvement of comprehensive efficiency in electro-Fenton. J Hazard Mater. 2021;412:125195. https://doi.org/10.1016/j.jhazmat.2021.125195.
78. Dong P, Wang H, Liu W, Wang S, Wang Y, Zhang J, Lin F, Wang Y, Zhao C, Duan X, Wang S, Sun H. Quasi-MOF derivative-based electrode for efficient electro-Fenton oxidation. J Hazard Mater. 2021;401:123423. https://doi.org/10.1016/j.jhazmat.2020.123423.
79. Caban M, Stepnowski P. How to decrease pharmaceuticals in the environment? A review. Environ Chem Lett. 2021;19:3115–38. https://doi.org/10.1007/s10311-021-01194-y.
80. Prathiba S, Kumar PS, Vo DVN. Recent advancements in microbial fuel cells: a review on its electron transfer mechanisms, microbial community, types of substrates and design for bio-electrochemical treatment. Chemosphere. 2022;286:131856. https://doi.org/10.1016/j.chemosphere.2021.131856.
81. Massazza D, Robledo AJ, Simon CNR, Busalmen JP, Bonanni S. Energetics, electron uptake mechanisms and limitations of electroautotrophs growing on biocathodes: a review. Bioresour Technol. 2021;342:125893. https://doi.org/10.1016/j.biortech.2021.125893.
82. Yang F, Zhai W, Li Z, Huang Y, Manzoor M, Yang B, Hou Y, Lei L, Tang X. Immobilization of lead and cadmium in agricultural soil by bioelectrochemical reduction of sulfate in underground water. Chem Eng J. 2021;422:130010. https://doi.org/10.1016/j.cej.2021.130010.
83. Yuan J, Ding Z, Bi Y, Li J, Wen S, Bai S. Resource utilization of acid mine drainage (AMD): a review. Water. 2022;14:2385. https://doi.org/10.3390/w14152385.
84. Yang M, Zhang X, Sun Y. Remediation of Cr(VI) polluted groundwater using zero-valent iron composites: preparation, modification, mechanisms, and environmental implications. Molecules. 2024;29:5697. https://doi.org/10.3390/molecules29235697.
85. Acharyya S, Das A, Thaker TP. Remediation processes of hexavalent chromium from groundwater: a short review. Aqua Water Infrastruct Ecosyst Soc. 2023;72:648–62. https://doi.org/10.2166/aqua.2023.123.
86. Irshad MA, Sattar S, Nawaz R, Al-Hussain SA, Rizwan M, Bukhari A, Waseem M, Irfan A, Inam A, Zaki MEA. Enhancing chromium removal and recovery from industrial wastewater using sustainable and efficient nanomaterial: a review. Ecotoxicol Environ Saf. 2023;263:115231. https://doi.org/10.1016/j.ecoenv.2023.115231.

87. Boruah H, Tyagi N, Gupta SK, Chabukdhara M, Malik T. Understanding the adsorption of iron oxide nanomaterials in magnetite and bimetallic form for the removal of arsenic from water. Front Environ Sci. 2023;11:1104320. https://doi.org/10.3389/fenvs.2023.1104320.
88. Hassan HR. A review on different arsenic removal techniques used for decontamination of drinking water. Environ Pollut Bioavailab. 2023;35:2165964. https://doi.org/10.1080/26395940.2023.2165964.
89. Wang H, Zhai P, Long X, Ma J, Li Y, Liu B, Xu Z. Research progress on using biological cathodes in microbial fuel cells for the treatment of wastewater containing heavy metals. Front Microbiol. 2023;14:1270431. https://doi.org/10.3389/fmicb.2023.1270431.
90. Sun Y, Wang H, Long X, Xi H, Biao P, Yang W. Advance in remediated of heavy metals by soil microbial fuel cells: mechanism and application. Front Microbiol. 2022;13:997732. https://doi.org/10.3389/fmicb.2022.997732.
91. Chen X, Teng W, Fan J, Chen Y, Ma Q, Xue Y, Zhang C, Zhang WX. Enhanced degradation of micropollutants over iron-based electro-Fenton catalyst: cobalt as an electron modulator in mesochannels and mechanism insight. J Hazard Mater. 2022;427:127896. https://doi.org/10.1016/j.jhazmat.2021.127896.
92. Arulmani SRB, Dai J, Li H, Chen Z, Sun W, Zhang H, et al. Antimony reduction by a non-conventional sulfate reducer with simultaneous bioenergy production in microbial fuel cells. Chemosphere. 2022;291:132754. https://doi.org/10.1016/j.chemosphere.2021.132754.
93. Singh A, Kaushik A. Removal of Cd and Ni with enhanced energy generation using biocathode microbial fuel cell: insights from molecular characterization of biofilm communities. J Clean Prod. 2021;315:127940. https://doi.org/10.1016/j.jclepro.2021.127940.
94. Zhao S, Chen Z, Khan A, Wang J, Kakade A, Kulshrestha S, et al. Elevated Cr(VI) reduction in a biocathode microbial fuel cell without acclimatization inversion based on strain Corynebacterium vitaeruminis LZU47-1. Int J Hydrogen Energy. 2021;46:3193–203. https://doi.org/10.1016/j.ijhydene.2020.05.254.
95. Liu SH, Huang WJ, Lin CW, Zhu TJ. Copper removal and microbial community analysis in a single medium sediment microbial fuel cell. J Water Process Eng. 2021;44:102348. https://doi.org/10.1016/j.jwpe.2021.102348.
96. Lin CW, Lai CY, Liu SH, Chen YR, Alfanti LK. Enhancing bioelectricity generation and removal of copper in microbial fuel cells with a laccase-catalyzed biocathode. J Clean Prod. 2021;298:126726. https://doi.org/10.1016/j.jclepro.2021.126726.
97. Hidayat ARP, Widyanto AR, Asranudin A, Ediati R, Sulistiono DO, Putro HS, et al. Recent development of double chamber microbial fuel cell for hexavalent chromium waste removal. J Environ Chem Eng. 2022;10:107505. https://doi.org/10.1016/j.jece.2022.107505.
98. Wang Y, Li W, Li H, Ye M, Zhang X, Gong C, Zhang H, Wang G, Zhang Y, Yu C. Fe/Fe3C@CNTs anchored on carbonized wood as both self-standing anode and cathode for synergistic electro-

Fenton oxidation and sequestration of As(III). Chem Eng J. 2021;414:128925. https://doi.org/10.1016/j.cej.2021.128925.

99. Zhao K, Quan X, Su Y, Qin X, Chen S, Yu H. Enhanced chlorinated pollutant degradation by the synergistic effect between dechlorination and hydroxyl radical oxidation on a bimetallic single-atom catalyst. Environ Sci Technol. 2021;55:14194–203. https://doi.org/10.1021/acs.est.1c04943.
100. Eljamal O, Eljamal R, Maamoun I, Khalil AME, Shubair T, Falyouna O, Sugihara Y. Efficient treatment of ammonia-nitrogen contaminated waters by nano zero-valent iron/zeolite composite. Chemosphere. 2022;287:131990. https://doi.org/10.1016/j.chemosphere.2021.131990.
101. Li Q, Chen Z, Wang H, Yang H, Wen T, Wang S, Hu B, Wang X. Removal of organic compounds by nanoscale zero-valent iron and its composites. Sci Total Environ. 2021;792:148546. https://doi.org/10.1016/j.scitotenv.2021.148546.
102. Visentin C, Trentin AWS, Braun AB, Thomé A. Life cycle sustainability assessment of the nanoscale zero-valent iron synthesis process for application in contaminated site remediation. Environ Pollut. 2021;268:115915. https://doi.org/10.1016/j.envpol.2020.115915.
103. Visentin C, Braun AB, Reginatto C, Cecchin I. Are contaminated soil and groundwater remediation with nanoscale zero-valent iron sustainable? An analysis of case studies. Environ Pollut. 2024;352:124167. https://doi.org/10.1016/j.envpol.2024.124167. (check full author list).
104. Zeng G, He Y, Wang F, Luo H, Liang D, Wang J, Huang J, Yu C, Jin L, Sun D. Toxicity of nanoscale zero-valent iron to soil microorganisms and related defense mechanisms: a review. Toxics. 2023;11:514. https://doi.org/10.3390/toxics11060514.
105. Yuan X, Li J, Lim JY, Zolfaghari A, Alessi DS, Wang Y, Wang X, Ok YS. Machine learning for heavy metal removal from water: recent advances and challenges. ACS ES&T Water. 2023. https://doi.org/10.1021/acsestwater.3c00215. 4:(add pages).

Figures

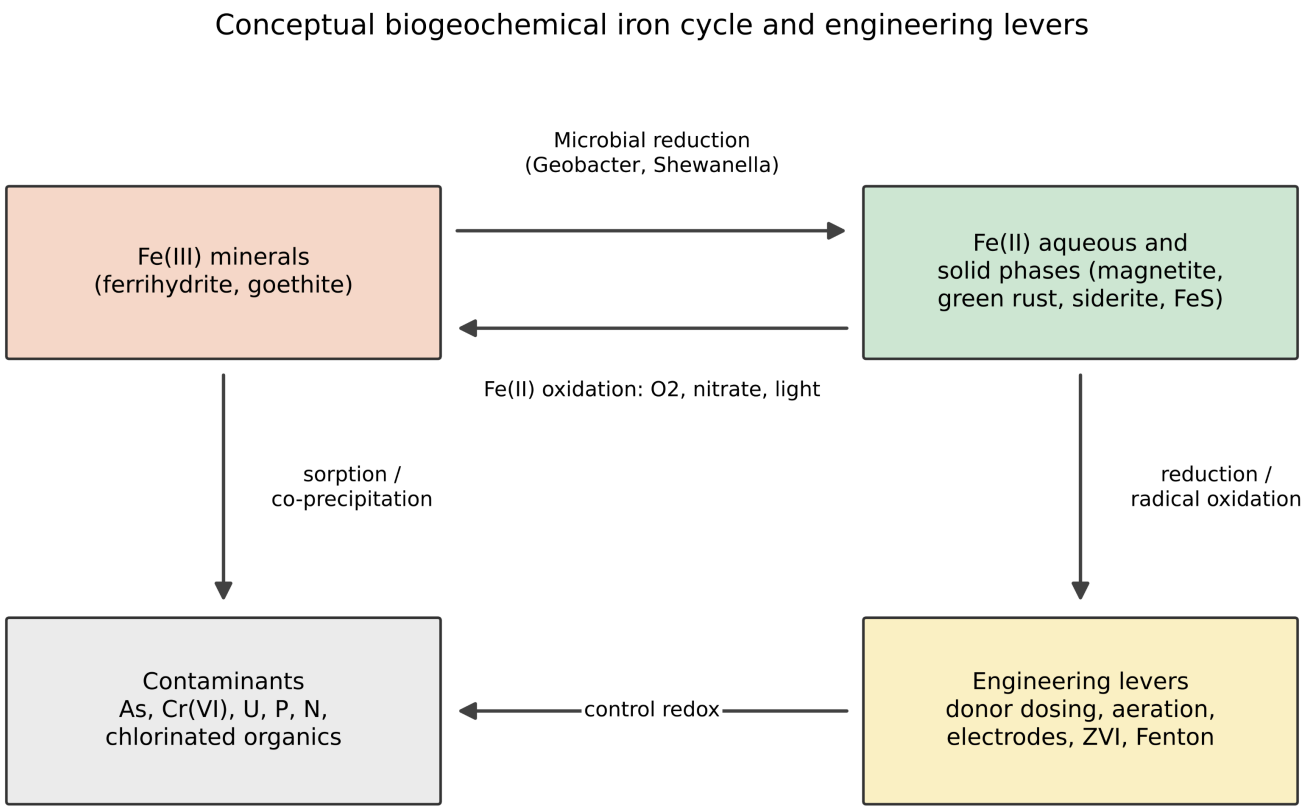


Figure 1

Conceptual schematic of the biogeochemical iron cycle: microbial reduction of Fe(III) minerals, Fe(II) oxidation by oxygen, nitrate, or light, interactions with contaminants, and the engineering levers used to steer redox conditions [1–3, 28, 40, 43–45, 49–51, 53].

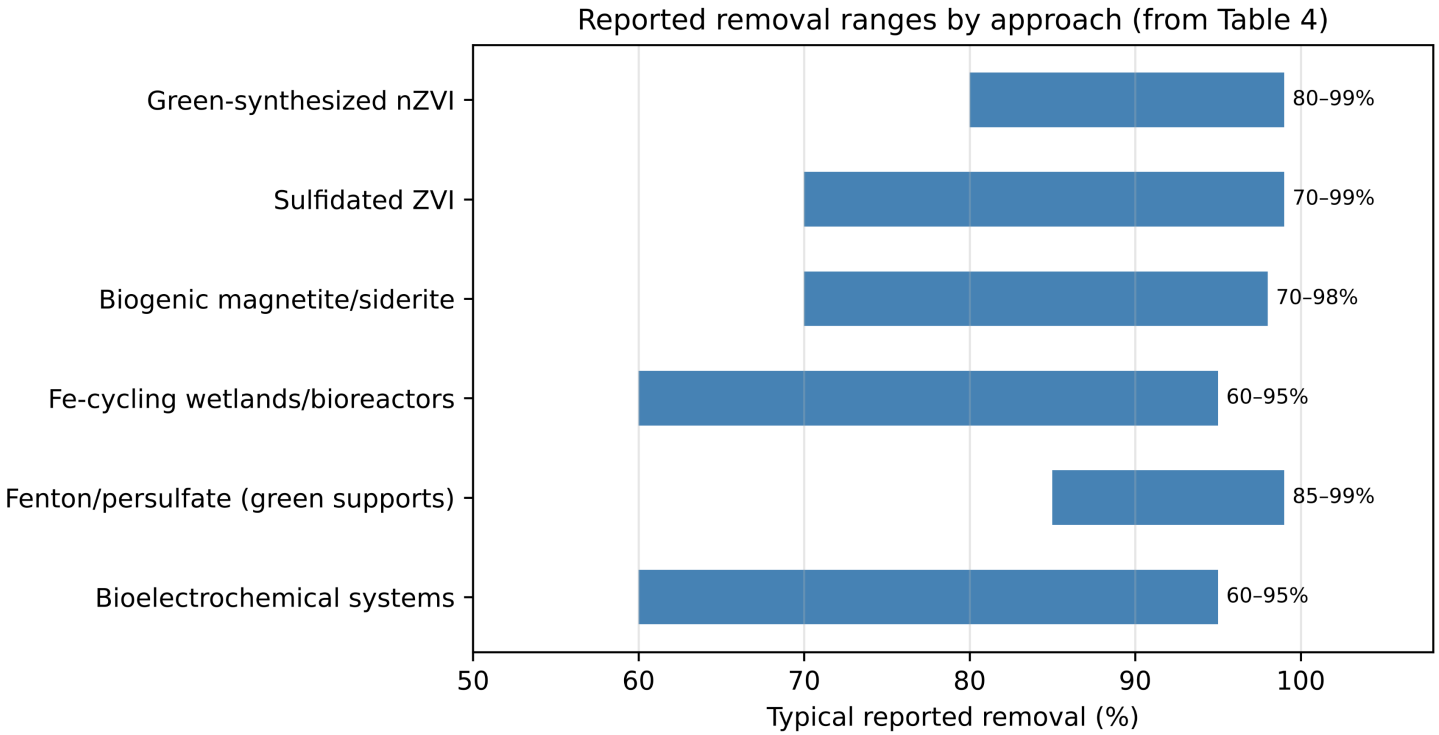


Figure 2

Reported removal ranges by approach, taken from the ranges summarized in Table 4 (green nZVI [19, 20, 31, 34, 49, 54, 84–86], sulfidated ZVI [20, 21, 28], biogenic minerals [13–15, 42, 51, 87, 88], Fe-cycling systems [13, 49, 51, 88], Fenton-type processes [28, 53, 70, 71], bioelectrochemical systems [44, 45, 89, 90]). PRBs are excluded because performance is field-dependent [38, 39, 54].

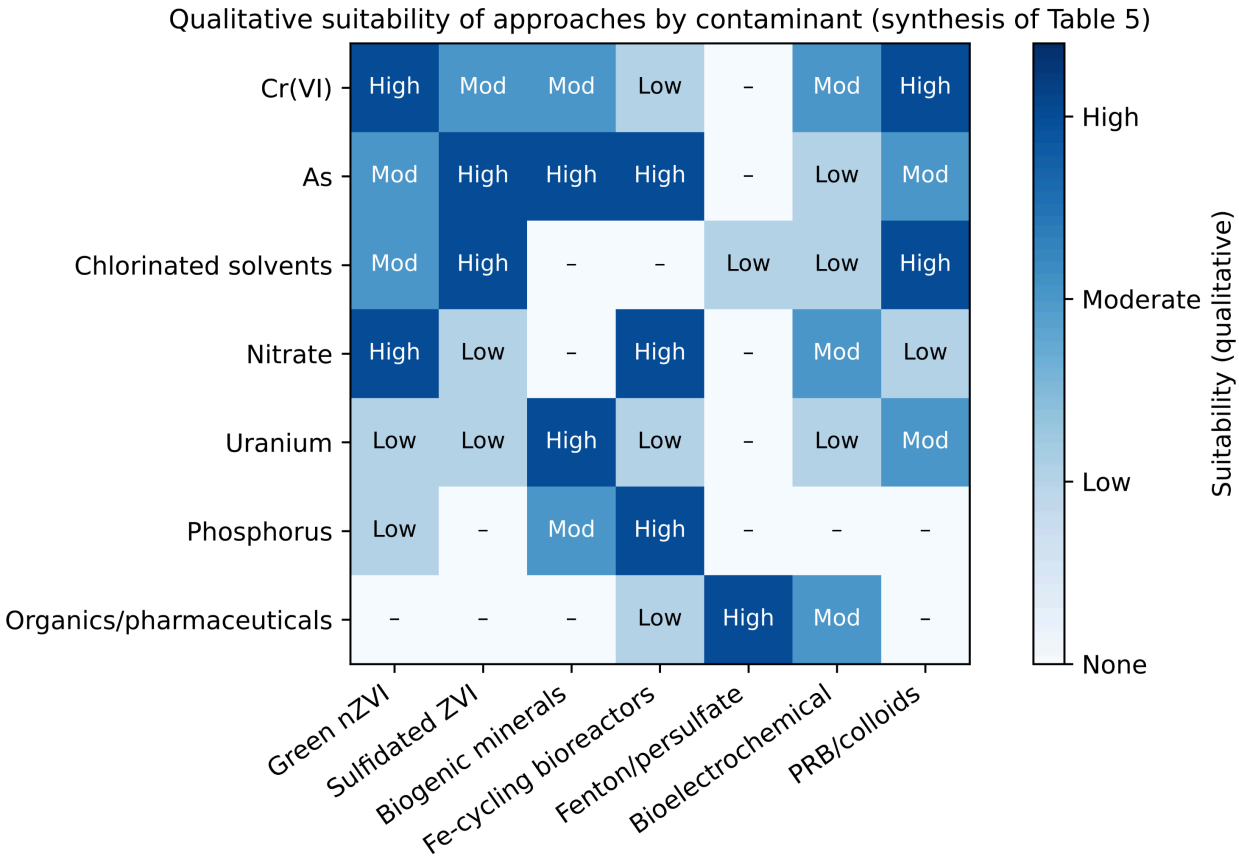


Figure 3

Qualitative suitability of iron-based approaches by contaminant class. Scores (none, low, moderate, high) are assigned by the author from the performance and mechanism evidence in Tables 4 and 5 and refs [13–15, 20, 21, 28, 34, 38, 39, 42, 49, 51, 53, 54, 70, 71, 84–88]; they are a synthesis aid, not measured values.

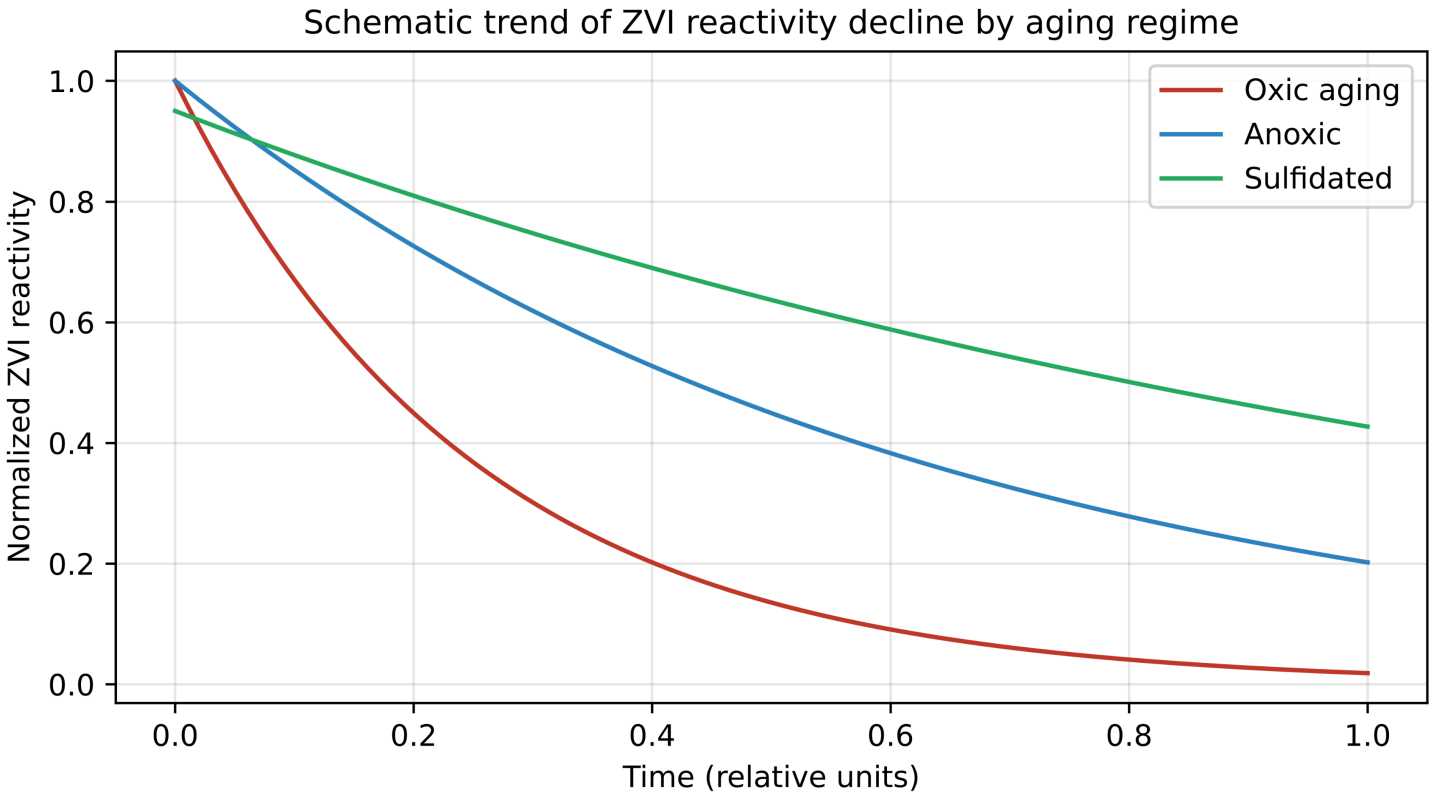


Figure 4

Schematic (illustrative, not fitted to data) of the trend in ZVI reactivity under oxic, anoxic, and sulfidated aging, summarizing qualitative findings in [19–21, 28, 34, 38, 39, 49, 54, 84–86].

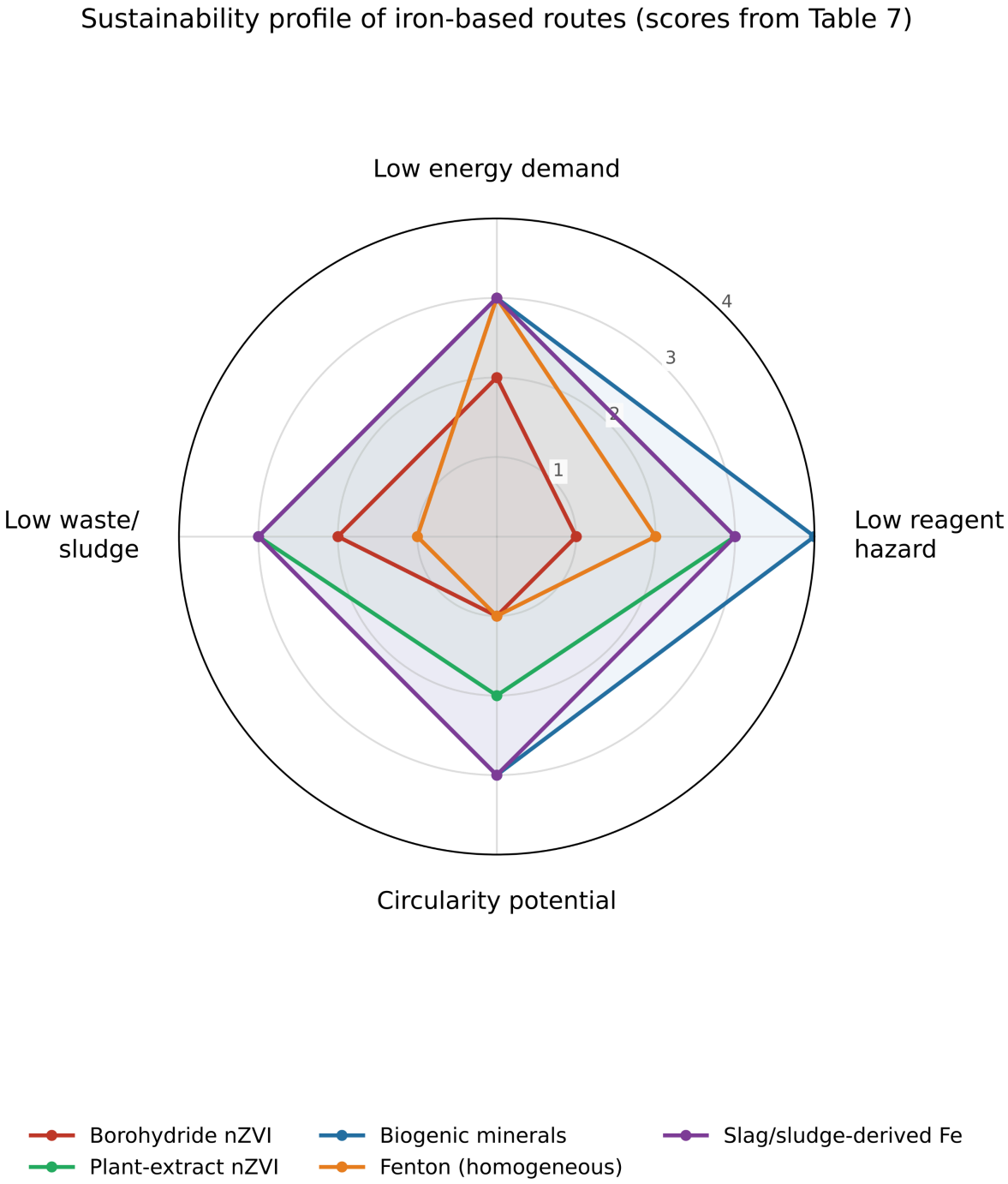


Figure 5

Radar chart of sustainability scores for five routes, with scores converted from the qualitative ratings in Table 7 (higher is more favorable; scale 1–4) [13–15, 19, 20, 28, 31, 34, 36, 37, 42, 49, 51, 53, 54, 70, 71, 84–88, 102, 103].

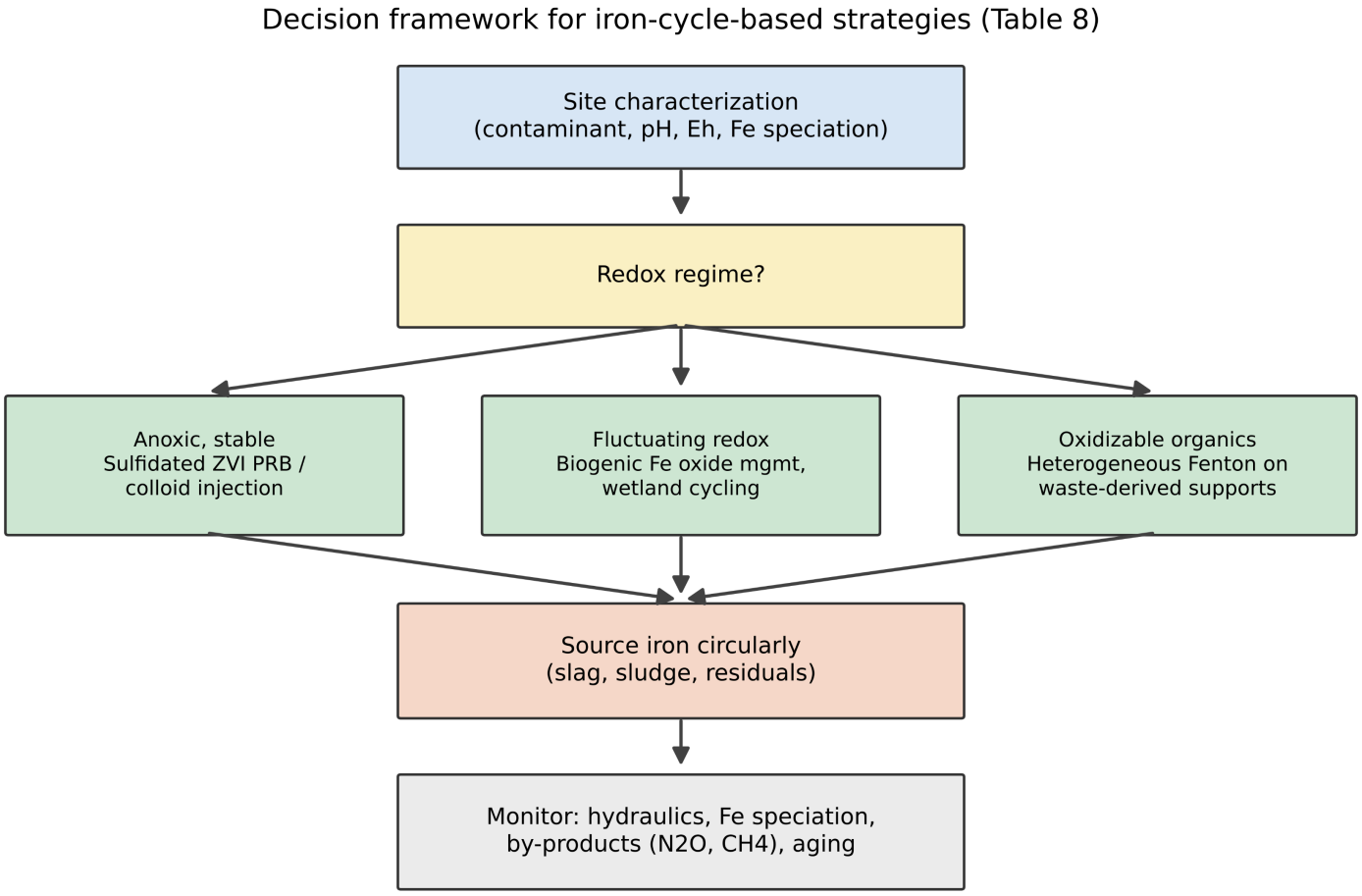


Figure 6

Decision framework from site characterization to technology selection and monitoring, corresponding to Table 8 [1, 13–15, 20, 21, 28, 36–42, 49, 51, 53, 54, 70, 71, 87, 88, 102, 103].